

Supporting Information

Electrochemical Size Measurement and Characterization of Electrodeposited Platinum Nanoparticles at Nanometer Resolution with Scanning Electrochemical Microscopy

Wei Ma^a, Keke Hu^b, QianJin Chen^a, Min Zhou^a, Michael V. Mirkin^b, Allen J. Bard^{a*}

^aCenter for Electrochemistry, Department of Chemistry, The University of Texas at Austin, Austin, Texas 78712, United States

^bDepartment of Chemistry and Biochemistry, Queens College, City University of New York, Flushing, New York 11367, United States

Table of Contents

1. EXPERIMENTAL SECTION -----	2
Chemicals and Materials -----	2
Pt UME Fabrication -----	2
C UME Fabrication -----	2
FIB-milled UME Characterization -----	3
Deposition of a PtNP or cluster on C UME -----	3
SECM Measurement -----	4
2. FIGURES -----	6
Figure S1-----	6
Figure S2-----	7
Figure S3 -----	8
Figure S4-----	10
Figure S5-----	11
Figure S6 -----	12

EXPERIMENTAL SECTION

Chemicals and Materials. Hexachloroplatinic acid (H_2PtCl_6), perchloric acid (HClO_4) and sodium perchlorate (NaClO_4) were purchased from Sigma-Aldrich and used as received. Ferrocenemethanol (FcMeOH , 97%, Acros Organics, NJ) were used after recrystallization. Hydrogen peroxide (H_2O_2), potassium nitrate (KNO_3) and sulfuric acid (H_2SO_4) were obtained from Fisher Scientific and used as received. A Milli-Q Integral system (EDM Millipore, Berllica, MA) was equipped to obtain ultrapure water with total organic carbon (TOC) level at <3 ppb as measured by an internally equipped TOC monitor as well as the resistivity $18.3 \text{ M}\Omega/\text{cm}$. All the solutions for electrochemical measurements were prepared with ultrapure water and filtrated by syringe filter with $0.1 \mu\text{m}$ diameter pore (Millex-Syringe driven filter unit, PVDF- $0.1 \mu\text{m}$, Merck Millipore Ltd.) except the acidic solution. All the glassware and the SECM cell made of Teflon and glass were extensively cleaned with piranha solution (3:1 ratio of H_2SO_4 : H_2O_2) followed by thorough washing with ultrapure water before use.

Pt UME Fabrication. A Pt UME was fabricated by using a CO_2 -laser puller, a microforge, and a focused ion beam (FIB) instrument. Briefly, a $25 \mu\text{m}$ diameter Pt wire (Goodfellow, annealed) inserted in the borosilicate capillary (I.D. 0.2 mm , O.D. 1 mm) was pulled together with CO_2 laser puller (P-2000, Sutter). Continuously, Pt UME was further annealed by Micro Forge (MF-900, Narishige, Tokyo, Japan) to decrease RG (a ratio between glass sheath and Pt radii) as well as a better sealing. A sharp tip with desirable inner and outer radii was obtained by FIB milling (SEM/FIB FEI Strata DB235 SEM/FIB with Zyvex S100).

C UME Fabrication. A cone-shaped nanopipette was pulled from a quartz capillary (O.D. 1.0 mm and I.D. 0.7 mm , Sutter Instrument, Novato, CA) and deposited with carbon by the chemical vapor deposition method. Briefly, a nanopipette with a tip diameter from 10 to 100 nm was fabricated by using a CO_2 laser puller (P-2000, Sutter Instrument) based on a program of HEAT = 800 , FIL = 4 , VEL = 22 , DEL = 128 , PUL = 110 and HEAT = 830 , FIL = 3 , VEL = 17 , DEL = 130 , PUL = 255 . A

nanopipette was nearly completely filled with carbon deposited using methane as the carbon source and argon as the protector for 1 hour at 900 °C. We used a copper nickel wire (0.13 mm diameter, Alfa Aesar, Ward Hill, PA) to establish a connection with a carbon nanotip for electrochemical measurements as well as its grounding to a sample stage in SEM, and FIB experiments and for protections from electrostatic damage. A C UME tip with a desirable radius was milled by using an FIB instrument to yield a flat tip.

FIB-milled UME Characterization. Electrochemical characterization of the obtained UMEs was performed by means of CV using a three-electrode configuration, where UME, silver/silver chloride electrode (Ag/AgCl), and Pt wire electrode are working, reference, and counter electrodes, respectively. Assuming a non-recessed, disk-shaped sub-micrometer electrode, estimation of the electrode radius can be done based on the steady-state current from CV at a scan rate of 100 mV·s⁻¹ in 0.5 mM FcMeOH aqueous solution containing 0.1 M KNO₃ as supporting electrolyte, as shown in Supporting Information, Figure S2. The radius for the FIB-milled UME was calculated based on the following formula:

$$i_{\text{lim}} = 4xnFDca$$

where i_{lim} is the steady-state current, x is a coefficient for the RG value, n is the number of electrons ($n = 1$ for FcMeOH oxidation), F is the Faraday constant (96485 C·mol⁻¹), D is the diffusion coefficient (7.6×10^{-6} cm²·s⁻¹ for FcMeOH in 0.1 M KNO₃ solution), c is the concentration of FcMeOH (0.5 mM), and a is the radius of the UME. This result was also further confirmed with an SEM image of the FIB-milled tip (Figure S2).

Deposition of a PtNP or cluster on C UME. A CHI760E bipotentiostat (CH Instrument, Austin, TX) was used for the electrodeposition of PtNP. To deposit a PtNP or cluster on the C UME, we used multiple potential step techniques in different concentration H₂PtCl₆ (100 μM; 30 μM; 10 μM) containing 10 mM H₂SO₄ solution, jumping the potential from a value (+0.45 V vs Ag/AgCl) where no reaction occurred

to driving potentials 0 V vs Ag/AgCl for different intervals for PtNP deposition (3-10 s) and then back to + 0.45 V vs Ag/AgCl. For this potential control, “return to the initial potential after run” function were used.

Nano-SECM Measurement. SECM experiments were carried out using a home-built instrument composed of a CHI760E bipotentiostat (CH Instrument) and a stage equipped with piezoelectric actuators (PI instruments) with a LabVIEW software. Notably, the positioning of the piezo and the electrochemistry are carried out independently using two different circuits. For the electrochemistry, a four electrode cell configuration was used in SECM experiments: a FIB-milled Pt UME or C UME with small RG served as the tip, which was mounted facing downward to a = 12.5 μm radius Pt UME substrate electrode. A Pt wire was used as a counter electrode and an Ag/AgCl electrode acted as a reference electrode, respectively. Particularly, to avoid electrochemical damage of nanometer-sized PtNP and electrode during electrochemical measurements, all relay switches in CHI760E bipotentiostat were physically removed following manufacturer’s instruction. Moreover, we handled both tip and substrate with protection tools as well as “cell on between runs” function by CHI software during the entire experiments. To suppress a thermal drift, all measurements were performed in an isothermal chamber with a faraday cage and a vibration isolation table. All of the metal parts in the vibration isolation table and the electronic equipment are grounded to prevent the electrochemical damage of the tip. Combined with CCD camera microscopy (Infinity2-1, Caltex lens VZ-400, Ontario, Canada), an UME used as SECM tip was aligned to 12.5 μm radius Pt substrate with a typical SECM imaging of substrate generation/tip collection (SG/TC) model. The tip was then brought closer to the Pt substrate with the SECM approach curve technique until the positive feedback current was observed in 0.5 mM FcMeOH solution containing 0.1 M KNO_3 . Then, the tip could be positioned ca. 20 μm above the substrate after 2–3 times of SECM approach with manipulating lockable differential micro-positioner in the z-axis, where the z-piezoelectric actuator has enough room to expand. After confirming a stable tip current level at the constant approached height,

thus forming a stable nanogap with a drift level <0.5 nm/min, UME tip was withdrawn to the initial position “0” of PIMikroMove (PI) to eliminate drift from piezo in the next electrochemical deposition experiment.

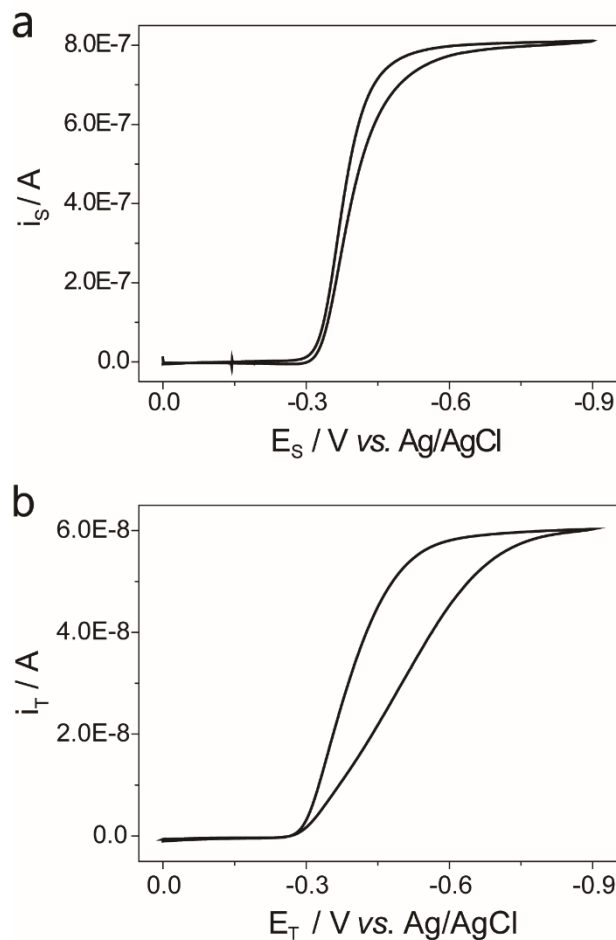


Figure S1. CVs of a = 12.5 μm Pt substrate (a) and a = 1.0 μm Pt tip (b) in 20 mM HClO_4 containing 0.1 M NaClO_4 as supporting electrolyte at a scan rate of 100 $\text{mV}\cdot\text{s}^{-1}$.

A steady-state current was obtained for radius 12.5 μm Pt substrate at potentials more negative than -0.5 V vs Ag/AgCl (Figure S1a), indicating a diffusion-controlled current produced by proton reduction. However, a clear reduction features was observed for radius 1.0 μm Pt tip, relating to H^+ reduction to H_2 , with a significant hysteresis corresponding to a Pt deactivation process on the reverse sweep (Figure S1b).

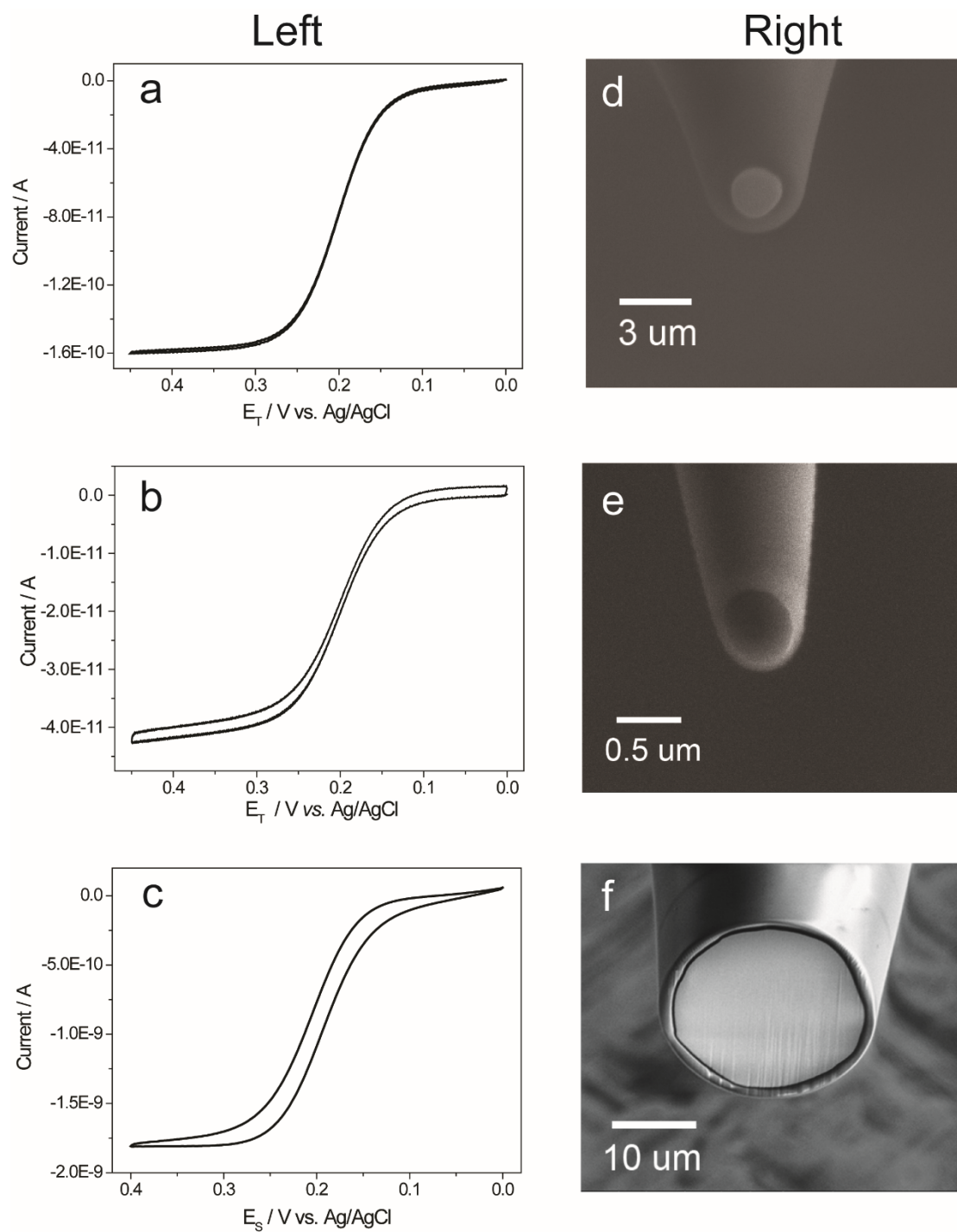


Figure S2. Left, CV of FIB-milled Pt tip (a); C UME tip (b); Pt substrate (c) in 0.5 mM FcMeOH solution containing 0.1 M KNO_3 ; the radius of the Pt microelectrodes are 0.97 μm , 0.26 μm and 11.8 μm based on steady-state current, respectively. Right, SEM image of FIB-milled Pt tip (d); C UME tip (e); Pt substrate (f) indicate the radii of the electrodes are 0.98 μm , 0.26 μm and 12.1 μm with very thin insulating sheath, respectively.

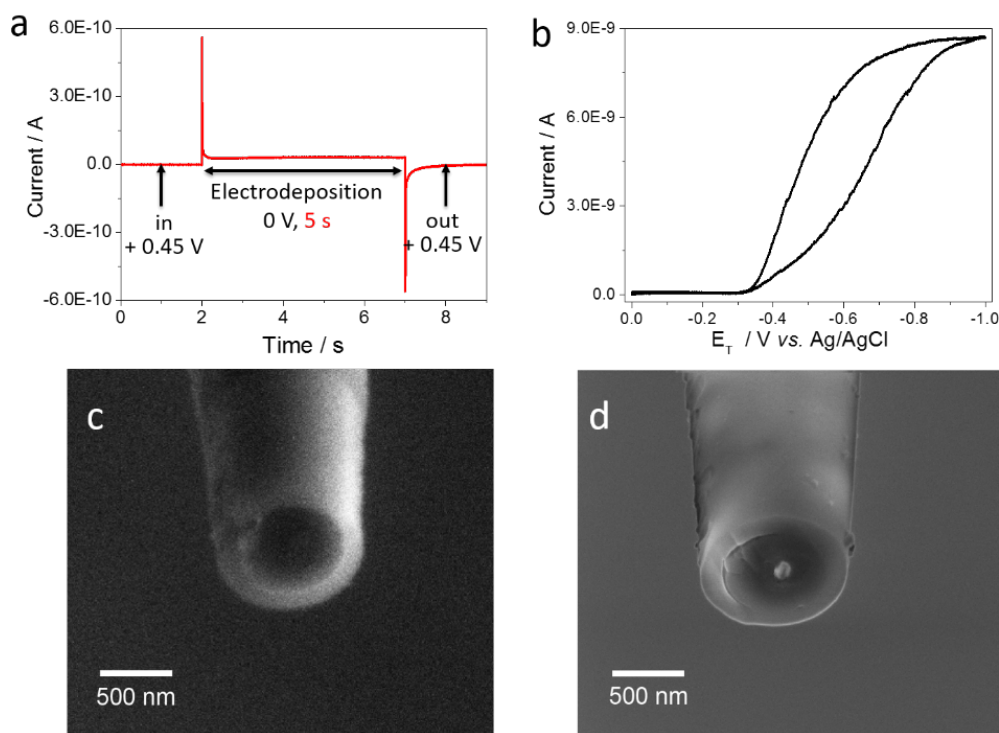


Figure S3. Voltammetric characterization of single PtNP size in 20 mM HClO₄ solution. (a) Current–time transients of the electrodeposition of a single PtNP on C UME for 5 sec in 100 μ M H₂PtCl₆ solution containing 10 mM H₂SO₄ at 0 V vs Ag/AgCl. (b) Cyclic voltammograms of a PtNP deposited C UME in 20 mM HClO₄ solution. (c-d) SEM image of C UME before and after deposition of a PtNP on C UME.

Voltammetric characterization of single PtNP size. We electrodeposited single PtNP at C UME by applying a pulsed potentiostat method.^{1,2} As displayed, the C UME surface was anodically protected at +450 mV vs Ag/AgCl during immersion in 100 μ M H₂PtCl₆ solution and prior to the application of a 0 V vs Ag/AgCl plating pulse to avoid the spontaneous deposition. After electrodeposition, the applied potential of the C UME was returned to the initial potential, +450 mV, for several seconds to completely stop the deposition process. A current–time transients for the electrodeposition of a single PtNP on C UME for 5 sec in 100 μ M H₂PtCl₆ solution containing 10 mM H₂SO₄ at 0 V vs Ag/AgCl was shown in Figure S3a. Typically, a falling current occurs at the beginning of the transients followed by a period over

which the current maintains a very low value and then current increase gradually, corresponding to H_2PtCl_6 diffusion to C UME surface and then the nucleation and the growth of a stable single PtNP.³ Assuming a spherical geometry and 100% deposition efficiency, we can estimate the size of deposited PtNP (r_{NP}) from the integrated charges through the equation below:

$$r_{\text{NP}} = \sqrt[3]{\frac{3QV_a}{4\pi nq}}$$

where r_{NP} is the radius of a PtNP, Q is the integrated charge from experimental current transient, V_a is the atomic volume of Pt ($2.32 \times 10^{-29} \text{ m}^3$), n is the number of electrons transferred per Pt atom ($n=4$), and q is the elementary charge. FIB-milled C UME offers a smooth and flat surface with a uniform conductivity across its surface.⁴ Additionally, our C UME tips with very small electroactive radii simplify the study of the nucleation and growth mechanism makes it possible to form only one single growth center and to allow that center to grow independently. Single Pt NP of ca. 64 nm radius on CUME was observed with nearly spherical geometry by SEM (Figure S3d). Notably, the observed dimension is close to the estimated size from the integrated charge of electrodeposition, 65 nm, indicating that most of transient currents could be attributed to the formation and growth of a PtNP (Figure S3a).

We further electrochemically characterized PtNP at C UME by steady-state voltammetry of HER in 20 mM HClO_4 containing 0.1 M NaClO_4 . A steady-state current with a significant hysteresis was obtained at potentials more negative than $-0.6 \text{ V vs Ag/AgCl}$ (Figure S3b), corresponding to a diffusion-controlled current produced by proton reduction. The radius of deposited Pt NP, r_{NP} , on the C UME surface was estimated from the steady-state current obtained voltammograms in HClO_4 solution assuming a single Pt NP with a spherical geometry on a planar surface, $i_{\text{lim}} = 4\pi(\ln 2)nFDCr_{\text{NP}}$, where i_{lim} is a steady-state current, n is the electron transfer number ($=1$ for proton reduction), F is the Faraday constant (96485 C/mol), D is the diffusion coefficient of H^+ ($8 \times 10^{-5} \text{ cm}^2/\text{s}$), and c is the concentration of proton (20 mM). In this case, the steady-state current of H^+ reduction at $-1.0 \text{ V vs Ag/AgCl}$ was 8.7 nA, and the radius of PtNP was calculated to be 63 nm. Notably, the estimated

size is in good agreement with both the integrated charge and the SEM result, indicating the validity of determined PtNP size by a steady-state current of HER.

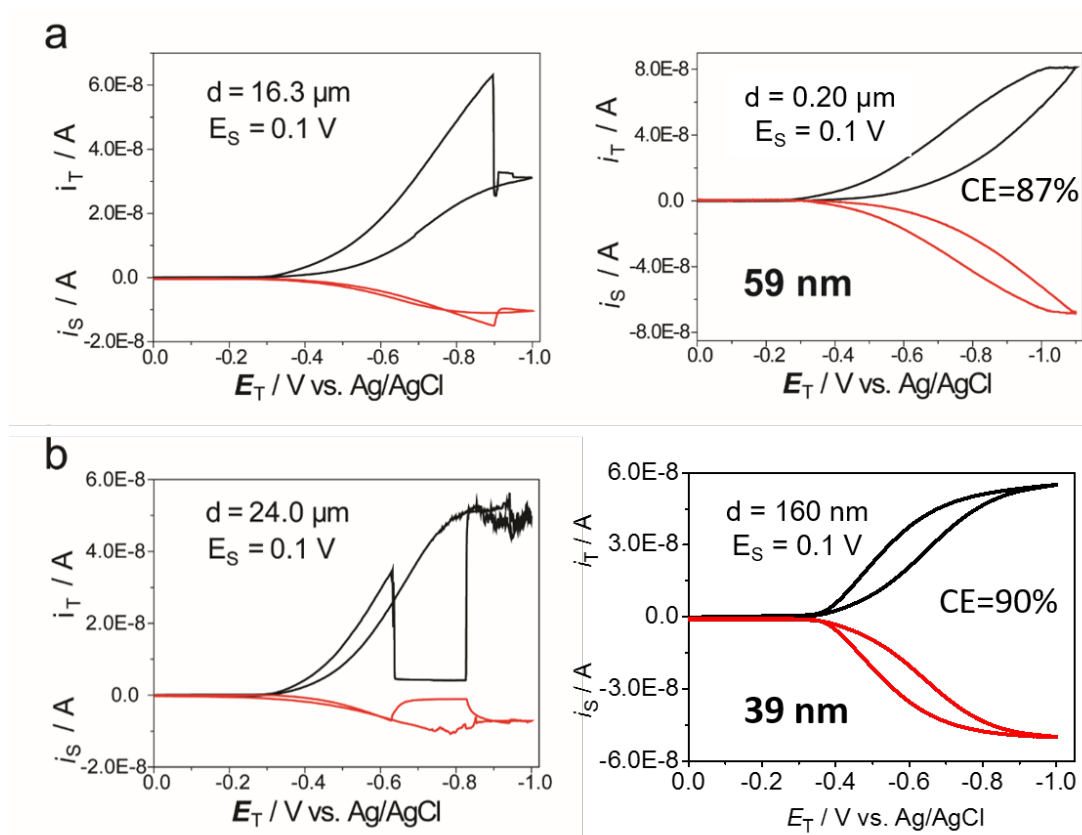


Figure S4. Generation and removal of H_2 bubble on C UME after electrodeposition of a single PtNP for (a) 5 sec and (b) 3 sec in $100 \mu\text{M}$ H_2PtCl_6 solution containing 10 mM H_2SO_4 at 0 V vs Ag/AgCl at different distances in an oxygen free 200 mM HClO_4 solution using the SG/TC mode of SECM. For SG/TC mode of SECM, the E_T is scanned from 0 to -1.0 V vs Ag/AgCl at a scan rate of $100 \text{ mV}\cdot\text{s}^{-1}$, while E_S is fixed at $+0.1 \text{ V}$ vs Ag/AgCl. Curves with black color and red color are the tip and substrate voltammograms, respectively.

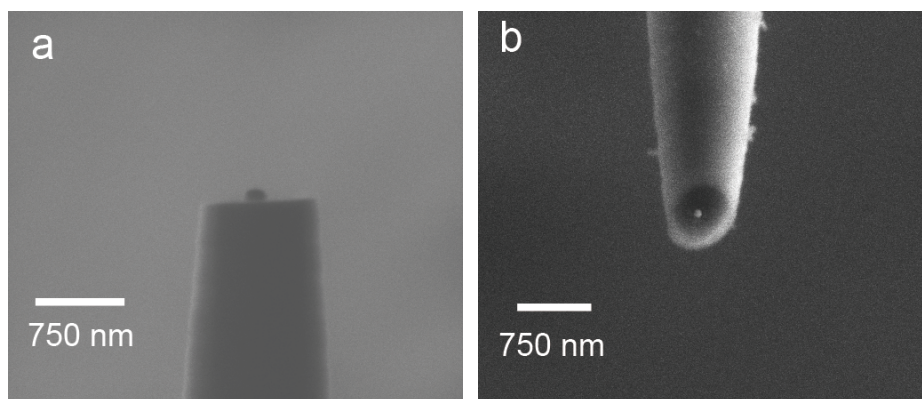


Figure S5. SEM image of C UME after deposition of single Pt NPs for (a) 5 sec and (b) 3 sec in 100 μM H_2PtCl_6 solution containing 10 mM H_2SO_4 at 0 V vs Ag/AgCl.

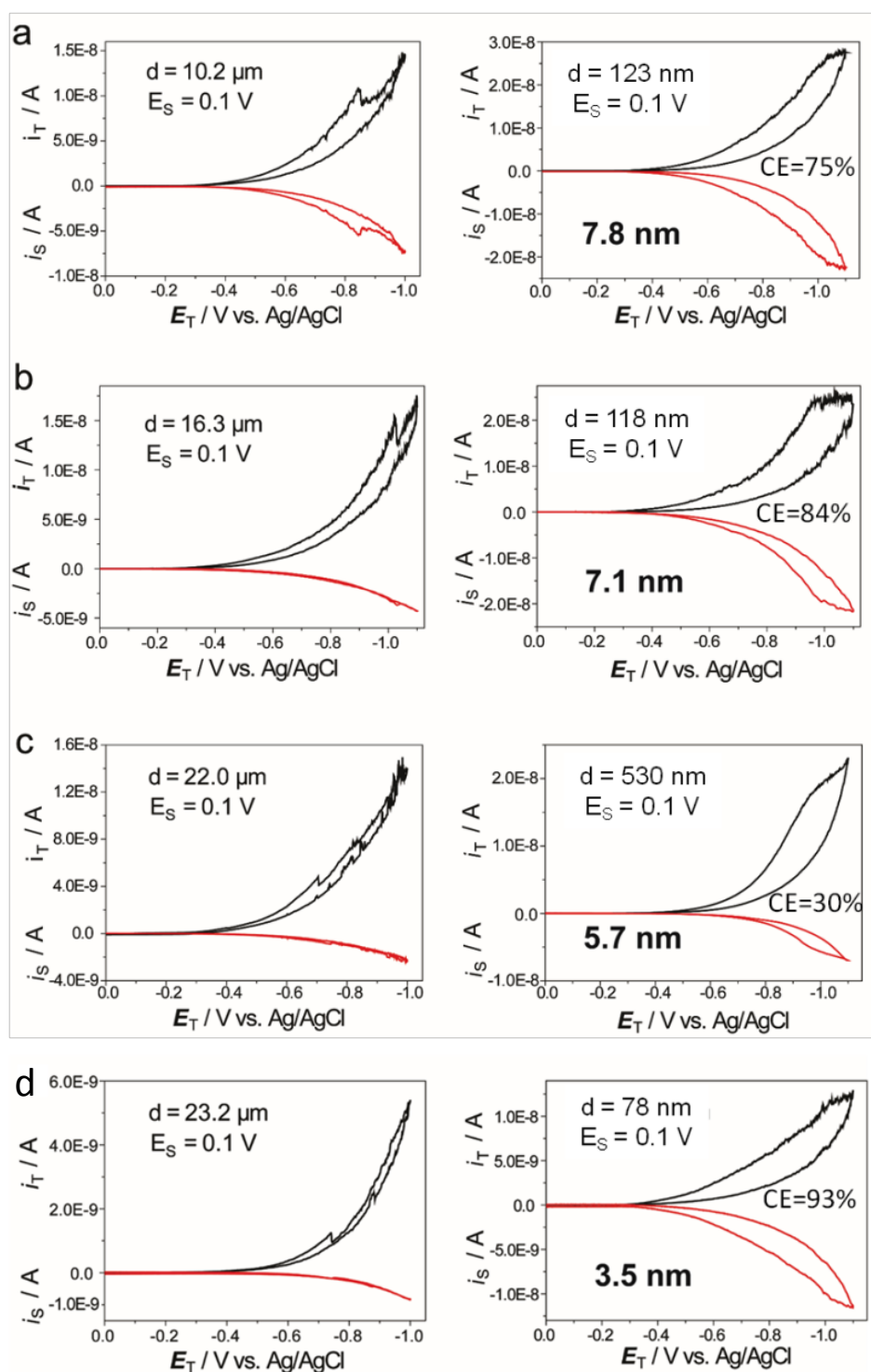


Figure S6. Generation and removal of H₂ bubble on C UME after electrodeposition of a single PtNP for 10 sec in (a-c) 30 μM (d) 10 μM H₂PtCl₆ solution containing 10 mM H₂SO₄ at 0 V vs Ag/AgCl at different distances in an oxygen free 500 mM HClO₄ solution using the SG/TC mode of SECM. For SG/TC mode of SECM, the E_T is scanned from 0 to -1.1 V vs Ag/AgCl at a scan rate of 100 mV·s⁻¹, while E_S is fixed

at +0.1 V vs Ag/AgCl. Curves with black color and red color are the tip and substrate voltammograms, respectively.

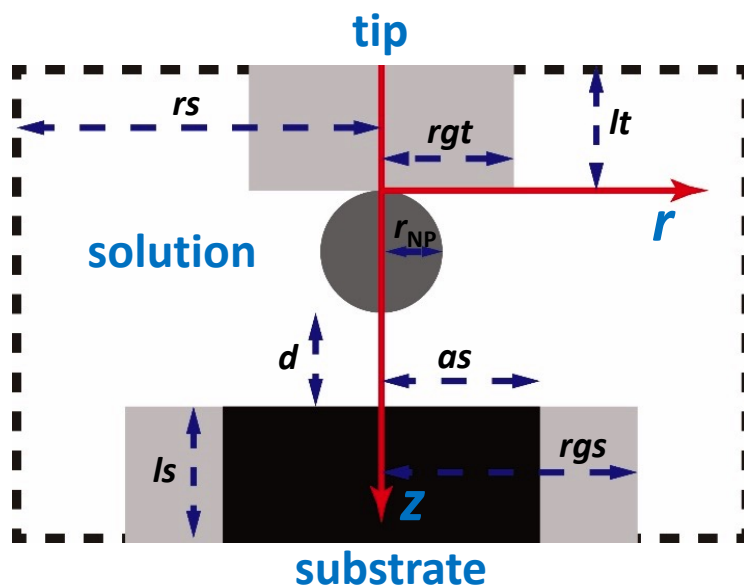


Figure S7. Geometry of the simulation space and parameters defining the diffusion problem for a sphere-shaped SECM tip approaching an inlaid disk substrate.

The steady-state diffusion problem for the tip generation and substrate collection (TG-SC) mode of the SECM operation is formulated for the diffusion-controlled reduction of proton ions (species 1) at the sphere-shaped tip and oxidation of hydrogen products (species 2) at the inlaid disk substrate, as shown in Figure S6. For simplicity, the “ $\frac{1}{2}\text{H}_2$ ” is taken as “species 2” in the electrode reaction and the involved formulation.



In this case, it must be aware that the real concentration of H_2 should be $\frac{1}{2}$ of the simulated value of “species 2”.

Then, the above diffusion problem can write in cylindrical coordinates as:

$$\frac{\partial^2 c_1}{\partial r^2} + \frac{1}{r} \frac{\partial c_1}{\partial r} + \frac{\partial^2 c_1}{\partial z^2} = 0 \quad (1.2)$$

$$\frac{\partial^2 c_2}{\partial r^2} + \frac{1}{r} \frac{\partial c_2}{\partial r} + \frac{\partial^2 c_2}{\partial z^2} = 0 \quad (1.3)$$

where r and z are the spatial coordinates and $c_i(r, z)$ is the concentration of the solution species.

The dimensionless variables are introduced as:

$$R = r / r_{NP} \quad (1.4)$$

$$Z = z / r_{NP} \quad (1.5)$$

$$C(R, Z) = c(r, z) / c_b \quad (1.6)$$

$$AS = as / r_{NP} \quad (1.7)$$

$$RGT = rgt / r_{NP} \quad (1.8)$$

$$RGS = rgs / r_{NP} \quad (1.9)$$

$$L = d / r_{NP} \quad (1.10)$$

$$LT = lt / r_{NP} \quad (1.11)$$

$$LS = ls / r_{NP} \quad (1.12)$$

where r_{NP} is the radius of the sphere-shaped tip, C_b is the bulk concentration, as is the radius of the inlaid disk substrate, rgt and rgs are the tip and substrate insulator radiuses, rs is the simulation space limit in the radial direction, lt and ls are the z-coordinates of the lower and upper simulation space limits, and d is the vertical distance from the sphere top to the substrate.

The dimensionless parameters are used as described in the formulation for the following diffusion problem:

$$\frac{\partial^2 C_1}{\partial R^2} + \frac{1}{R} \frac{\partial C_1}{\partial R} + \frac{\partial^2 C_1}{\partial Z^2} = 0; \quad 0 \leq R < RS, \quad -LT < Z < 2 + L + LS \quad (1.13)$$

$$\frac{\partial^2 C_2}{\partial R^2} + \frac{1}{R} \frac{\partial C_2}{\partial R} + \frac{\partial^2 C_2}{\partial Z^2} = 0; \quad 0 \leq R < RS, \quad -LT < Z < 2 + L + LS \quad (1.14)$$

$$C_1 = 0, D_1 \frac{\partial C_1(R, Z)}{\partial n} + D_2 \frac{\partial C_2(R, Z)}{\partial n} = 0; \quad (\text{tip surface}) \quad (1.15)$$

$$0 \leq R \leq 1, Z = 1 \pm \sqrt{1 - R^2}$$

$$C_2 = 0, D_1 \frac{\partial C_1(R, Z)}{\partial n} + D_2 \frac{\partial C_2(R, Z)}{\partial n} = 0; \quad (\text{substrate surface}) \quad (1.16)$$

$$0 \leq R \leq AS, Z = 2 + L$$

where $\partial C_i(R, Z) / \partial n$ is the normal derivative and D_i is the diffusion coefficient of the species.

$$\frac{\partial C_1(R, Z)}{\partial n} = \frac{\partial C_2(R, Z)}{\partial n} = 0;$$

$$0 < R \leq RGT, Z = 0;$$

$$-LT \leq Z \leq 0, R = RGT; \quad (\text{insulating surface}) \quad (1.17)$$

$$AS < R \leq RGS, Z = 2 + L;$$

$$2 + L \leq Z \leq 2 + L + LS, R = RGS;$$

$$C_1 = 1, C_2 = 0;$$

$$-LT \leq Z \leq 2 + L + LS, R = RS; \quad (\text{simulation space limit}) \quad (1.18)$$

$$RGT < R \leq RS, Z = -LT;$$

$$RGS < R \leq RS, Z = 2 + L + LS$$

$$\frac{\partial C_1(R, Z)}{\partial n} = \frac{\partial C_2(R, Z)}{\partial n} = 0; R = 0, 2 \leq Z \leq 2 + L \quad (\text{axis of symmetry}) \quad (1.19)$$

The collection efficiency is defined as the ratio of the integrated diffusion flux of “species 2” over the substrate surface to the integrated diffusion flux of species 1 over the tip surface.

REFERENCE

- (1) Chen, S.; Kucernak, A. *J. Phys. Chem. B* **2003**, *107*, 8392-8402.
- (2) Kim, J.; Bard, A. J. *J. Am. Chem. Soc.* **2016**, *138*, 975-979.
- (3) Velmurugan, J.; Noel, J.-M.; Mirkin, M. V. *Chem. Sci.* **2014**, *5*, 189-194.
- (4) Chen, R.; Hu, K. K.; Yu, Y.; Mirkin, M. V.; Amemiya, S. *J. Electrochem. Soc.* **2016**, *163*, H3032-H3037.